Distortion reduction for spiral-fMRI: Comparison of iterative and non-iterative parallel imaging reconstruction algorithms

H. Schmiedeskamp[1,2], L. J. Pisani[2], C. Lui[2], C. Law[2], K. P. Pruessmann[1], G. H. Glover[2], and R. Bammer[2]

[1]Institute for Biomedical Engineering, ETH Zurich, Zurich, Switzerland, [2]Department of Radiology, Stanford University, Stanford, CA, United States

Introduction Single-shot spiral imaging is a very efficient technique to acquire dynamic data for fMRI experiments rapidly and has profound advantages over single-shot EPI as it distributes the burden over two gradient axes. Similar to EPI, spirals suffer from geometric image distortions, T2*-related blurring, and signal dropout/pile-up artifacts. Parallel imaging (PI) has shown great utility to counteract these issues by faster traversing through k-space at the cost of increased signal-to-noise ratio (SNR) and (in the case of non-Cartesian acquisitions) considerably increased reconstruction times. Specifically, CG SENSE [1] has been proposed as a robust, iterative PI reconstruction method for spiral data. However, its iterative fashion has two potential shortcomings: 1) prohibitively long reconstruction time for time-series imaging; 2) unknown number of iterations required to reach the optimal convergence. A reconstruction that determines the unfolding parameters upfront and applies it successively to all dynamic phases would be more desirable. Aside from spiral GRAPPA [2], which is currently rather limited in the use of possible trajectories, we have recently developed a non-iterative PI reconstruction method for arbitrary trajectories using k-space sparse matrices (kSPA) [3], which affords much faster reconstructions of dynamic time series. In this study, we assessed 1) conventional (R=1) and PI-accelerated (R=2) single-shot, variable density (VD) spiral fMRI for image distortion; 2) CG SENSE and kSPA for differences in image quality and fMRI activation.

Methods A T2*-weighted VD (pitch=2) spiral sequence was implemented on a 1.5T unit (GE Signa LX, 8channel MRI Devices coil) for performing the aforementioned comparisons. Scan parameters were as follows: matrix = 96×96, 24cm FOV, 5mm slices, skip 0.5mm, TR/TE = 2000/50ms, flip = 80°, RBW = +/-125kHz, number of slices = 17. Due to the shortened readout, R=2 afforded 22 slices per TR. To avoid signal fluctuation for R=2 between odd and even spiral interleaves, 2 sets of full interleaves were taken first for calibration purposes and scanning was then continued using only the even interleaf for the entire time series. A combined auditory and visual stimulus with 8 on/off-cycles of 48 seconds each was presented to each subject. In addition, the volunteers were asked to perform a bilateral finger-tapping experiment during the 24 seconds long on-periods. For postprocessing, the voxel-wise temporal signal curve was correlated with a sine wave (phase-offset adjusted in order to get maximal correlation using a similar method as described in [4]). The total number of activated voxels being above a linear correlation coefficient threshold of 0.35 were quantified and served as a metric for efficacy. The average SNR over all activated voxels and the average SNR as well as the SFNR (temporal SNR) over a non-activated ROI were determined for CG SENSE, kSPA as well as for the non-accelerated scan using the methods described by Glover et al. [4].

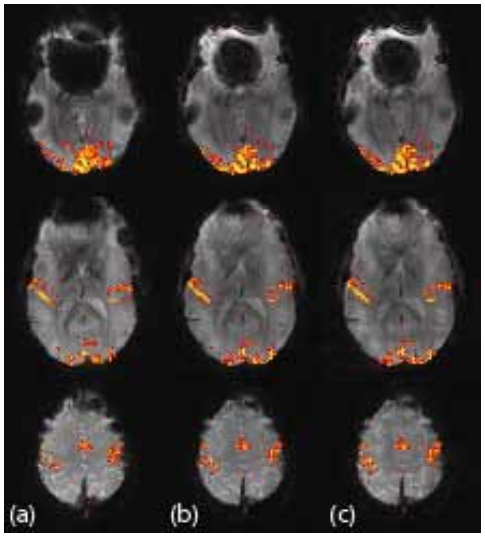

Fig. 1: Comparison of R=1 (a) to R=2 reconstructed using CG SENSE (b) and kSPA (c) for selected slices

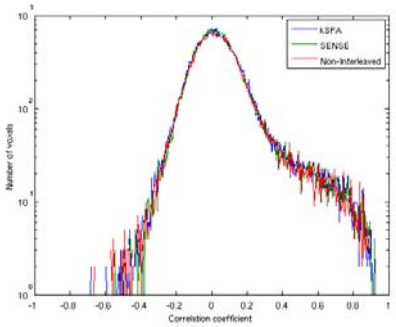

Fig. 2: Distribution of correlation coefficients of all acquired voxels within the brain

Results Considerable distortion reduction was achieved by using PI-accelerated VD spiral scans. Non-accelerated scans suffered from big signal dropouts, located mainly in frontal regions of the brain above the sinuses and near the auditory canals (Fig. 1). As expected, the SNR and SFNR of the accelerated scans were less than that of conventional VD spirals (Table 1). The distribution of activation patterns was very similar across all the three methods (Fig. 1). Interestingly, histograms of the correlation coefficient (Fig. 2) showed only minor differences with a slight tendency towards larger activation for the PI methods. Despite kSPA's 5-6 times faster reconstruction speed than CG SENSE no significant differences in activated voxels and marginal better SNR and SFNR were found (Table 1).

Table 1 – Comparison of different reconstruction methods and acceleration factors

	R=1	*R=2, CG SENSE*	*R=2, kSPA*
Nr of activated voxels	2124	2198	2317
SNR of activated areas *	1	0.72	0.76
SNR in non-activated ROI *	1	0.68	0.68
SFNR in non-activated ROI *	1	0.79 (± 0.11)	0.82 (± 0.12)

* SNR and SFNR normalized to R=1, standard deviation of SFNR indicated by brackets

Discussion This study demonstrated improved image quality with PI-accelerated scans and that kSPA can be used for fMRI image reconstruction of parallel acquired data without the reconstruction time penalty of CG SENSE. Here, kSPA showed activation pattern similar to CG SENSE that revealed a slightly larger number of activated voxels and better SNR in these regions. Compared to non-accelerated spiral imaging, the parallel acquisitions demonstrated less blurred activation and even a higher total number of activated voxels. This can be due to the fact that signal dropouts or distortions compromised the activation pattern of the R=1 data more than those acquired with R=2. In particular, the reduced T2* blurring helps to better localize activation, whilst the faster readout allows a larger spatial frequency range to be covered at instances when the BOLD contrast is optimal. Conversely, the numbers of activated voxels in R=1 scans could be slightly offset by increased spatial blurring of activation. In contrast to constant sampling density spirals, VD spirals require a longer readout time, leading to a potentially higher signal loss at higher spatial frequencies and greater sensitivity to off-resonances. However, VD sampling offers better navigation and self-calibration capabilities.

References [1] Pruessmann *et al.*, MRM 46:638-651,2001, [2] Heberlein *et al.*, MRM 55:619-625, 2006, [3] Lui C. *et al.*, MRM in review, [4] Glover *et al.*, MRM 39:361-368, 1998

Acknowledgements: This work was supported in part by the NIH (1R01EB002711), the Center of Advanced MR Technology at Stanford (P41RR09784), Lucas Foundation.